Reports

Hail Detection with a Differential Reflectivity Radar

Abstract. *A major objective in the remote sensing of convective storms by radar is the clear and reliable differentiation between regions of hail and regions of rainfall. This report describes the application of the differential reflectivity (Z_{DR}) radar technique to the problem of hail detection. The procedure is based on the markedly different polarization-dependent backscatter characteristics of rain and hail. Field experiments conducted in Colorado during the spring of 1983 provide significant evidence of hail detection with this new radar technique.*

Conventional incoherent meteorological radar measures the amount of backscattered power from precipitation particles (raindrops, hail, ice crystals) contained within a resolution volume determined by the range, antenna pattern, and transmitted pulse width. The backscattered power per unit volume is proportional to the reflectivity factor Z (in millimeters to the sixth power per cubic meter), which is often expressed in decibels above the reference value 1 mm^6 m^{-3}; that is, dBZ = 10 log (Z). The transmitted power is usually linearly polarized, and the received power is of the same polarization. Conventional radar measurements of reflectivity do not directly indicate the type of hydrometeors producing the radar signal except in a gross sense; for example, large hail often causes a higher reflectivity than rain.

The first attempts at distinguishing hailstorms from other types of storms used reflectivity measurements (*1*). This approach is based on an examination of the echo intensity and its structure and time evolution within a storm (*2*) and is currently being advocated for use as an automatic means of hail detection as part of the development, in the United States, of a Next-Generation Weather Doppler Radar (NEXRAD) (*3*). However, the procedure is very cumbersome and highly limited, since the algorithm determines only whether the storm contains hail. Information on the location and extent of the hailfall within the storm is not provided.

Another approach to hail detection is based on radar observations at two wavelengths (*4*). This technique depends upon the ratio of the echo power at 10- and 3-cm wavelengths and has also been implemented by Soviet researchers (*5*). A major factor complicating the interpretation of dual-wavelength measurements is rainfall attenuation (*6*). An alternative dual-wavelength approach postulates that the range derivative of the ratio of reflectivities at 10- and 3-cm wavelengths reduces the effects of attenuation on the smaller wavelength signal (*7*). However, problems such as mismatched antenna beam patterns at the two wavelengths (*8*) and the requirement for simultaneous operation of two radars have limited the utility of dual-wavelength procedures thus far.

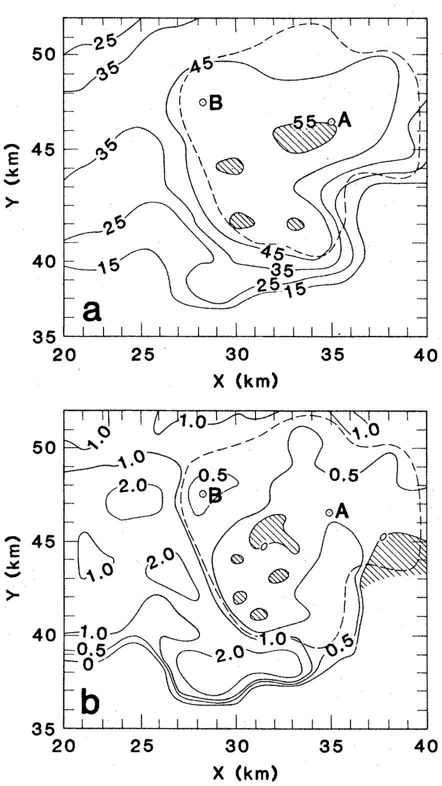

Fig. 1. The Z_H (a) and Z_{DR} (b) contours of a portion of the 4 June 1983 storm in Colorado at an altitude of 2.3 km above mean sea level between 5:13 and 5:21 p.m. Mountain Daylight Time (MDT). The Z_H contours are at 10-dB intervals, and the radar is located at (x, y) = (0, 0). There are small regions in excess of 55 dBZ. The Z_{DR} contours are in decibels with varying intervals defined by the levels 0, 0.5, 1.0, and 2.0 dB. Regions at and slightly below 0 dB are hatched. The extended hail region as estimated by the Z_{DR} hail signal is contoured by dashed lines in both (a) and (b).

During the early 1960's, Canadian researchers introduced a method that is based on the depolarization characteristics of hailstones as compared to raindrops and involves radar measurements of the complex backscatter coherency matrix with circular polarization used as a reference basis (*9, 10*). Complicating factors affecting the use of this method include propagation effects in rainfall (*11*), the need to maintain a high degree of isolation between polarization channels, and requirements on the sensitivity of the radar system (*9*).

The hail detection scheme reported here is based on the inherent differences in the radar cross sections of rain and hail at horizontal and vertical linear polarizations (*12*). Raindrops falling at terminal velocity in steady-state flow are nearly oblate spheroids because of a balance between gravity, surface tension, and aerodynamic forces. These observations were made above the surface boundary layer with a pair of two-dimensional precipitation probes (*13*) mounted on an aircraft with orthogonal optical axes so that it was possible to image the drops along two planes, that is, a plan view and a side view (*14*). Earlier observations and analyses indicate that (i) raindrops can be modeled as a collection of oblate spheroids with symmetry axes oriented vertically (*15, 16*) and (ii) the axial ratio of the equilibrium shapes is a function of raindrop size (*17*). Hence, the rain medium is anisotropic and the principal polarization vectors are closely aligned along the horizontal (H) and vertical (V) directions.

In contrast to the rain medium, the hail medium is significantly more isotropic because hail particles are irregular and generally nonspherical; oblate and conical shapes have been observed. In addition, hailstones often tumble with no strong orientation effect, thus appearing isotropic with respect to horizontal or vertical polarization states, or both. This behavior is consistent with the results of Canadian observers, which show that the degree of common alignment of hail is generally much smaller than that of rainfall (*16, 18*). There is also a tendency for Z to be greater than ~30 dBZ for hail, with the probability of hail increasing as opposed to the probability of rainfall decreasing as Z increases (*19*).

The dual-polarization radar technique for hail detection reported here is based on differential reflectivity: Z_{DR} = 10 log (Z_H/Z_V), where Z_H and Z_V are the radar reflectivity factors at horizontal and vertical polarizations, respectively (*12*). In rainfall regions, Z_{DR} is always positive and generally varies between 0 and 4 dB. Furthermore, Z_{DR} tends to be spatially correlated with absolute reflectivity (Z_H or Z_V). In hail regions Z_{DR} rapidly drops to values near 0 dB but exhibits larger positive values in the surrounding rain regions. On the other hand, in hail regions the reflectivity generally increases or maintains a relatively high value. This anticorrelated pattern defines the Z_{DR} hail signal. Thus the (Z_H and Z_{DR}) signals in rain and hail regions behave differently and can be used to discriminate between hail and rain regions.

The Z_{DR} technique was recently implemented on the CP-2 radar system operated by the Field Observing Facility of the National Center for Atmospheric Research (NCAR). The transmitted pulses are switched rapidly and sequentially between H and V polarizations with a high-power ferrite circulator; reception is copolar, yielding Z_H and Z_V, from which Z_{DR} is derived. This measurement scheme results in accurate estimates of Z_{DR} which, for the data presented here, have standard errors between 0.1 and 0.3 dB (*20*). Since reception is always copolar with respect to the transmitted polarization state, polarization purity of the antenna is not a major consideration. Moreover, system complexity is reduced since a dual-channel receiver is not necessary for the measurements (*21–23*).

Differential reflectivity measurements were made with the CP-2 radar during Project May Polarization Experiment (MAYPOLE), jointly conducted by Ohio State University, Colorado State University, and NCAR near Boulder, Colorado, from 1 May through 15 June 1983. This report highlights the real-time hail-detection feature of Z_{DR} on 4 and 8 June 1983.

On the afternoon of 4 June, hail cells were observed by radar and were confirmed by mobile hail chase teams and independent observers. Figure 1, a and b, shows constant-altitude plan-position-indicator (PPI) scans of Z_H and Z_{DR}, respectively. Regions of the Z_{DR} hail signal are contoured in Fig. 1. These are regions where (Z_H and Z_{DR}) signals are atypical of rainfall; that is, Z_{DR} is small and Z_H large. The contoured hail cell

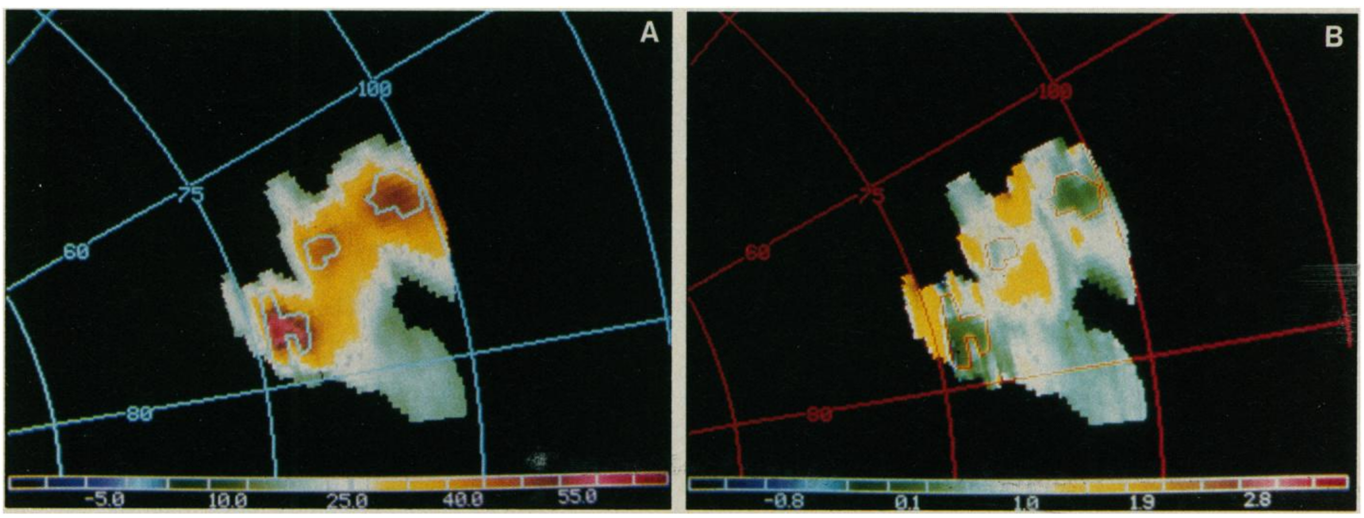

Fig. 2. The Z_H (A) and Z_{DR} (B) plan-position-indicator scans of the 8 June 1983 convective storm in Colorado at 8:18 p.m. MDT at an elevation angle of 0.5°. Radial distances (in kilometers) are noted by the circular arcs. Azimuth markings are in degrees clockwise from north. Note the contoured high-Z_H (greater than 50 dBZ) and low-Z_{DR} (0 to 0.4 dB) regions where the Z_{DR} signal predicts hail. These characteristics of this storm exhibit spatial continuity and are also observed in scans at other elevation angles.

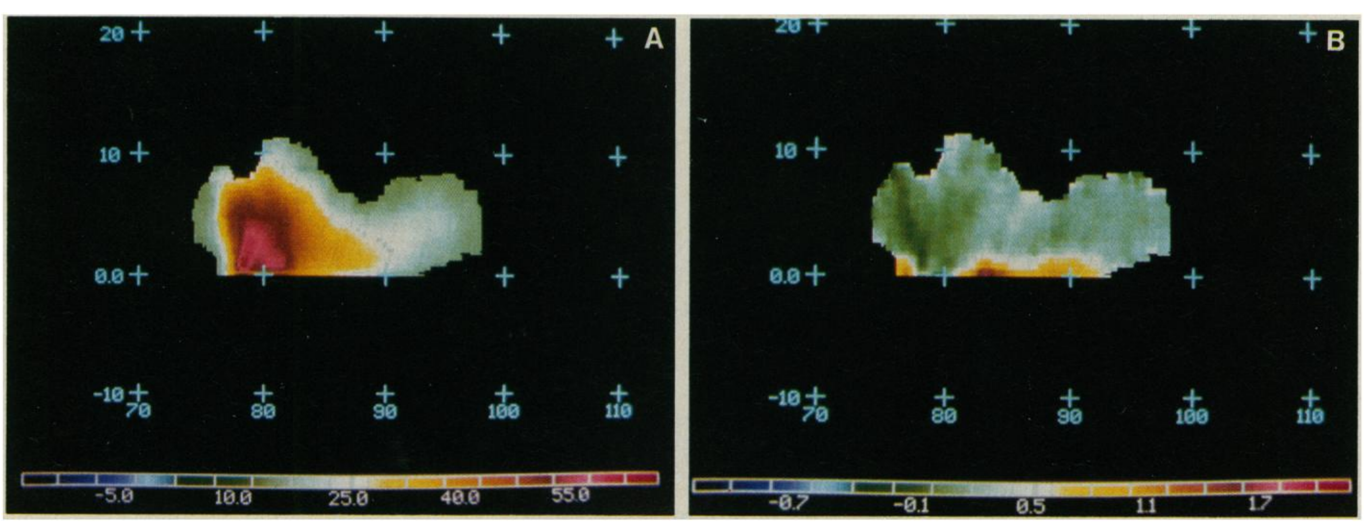

Fig. 3. Top and bottom and range-height-indicator profiles showing, respectively, the Z_H (A) and Z_{DR} (B) scans of a convective storm in Colorado on 8 June 1983 at 8:23 p.m. MDT The horizontal axis indicates distance from the radar (in kilometers), and the vertical axis is the height above ground. Note the clearly observable hailshaft located close to 80 km, where Z_{DR} is very close to 0 dB and Z_H is greater than 50 dBZ. The larger Z_{DR} values at lower heights are due to rain. There is a distinctive separation between water phase and ice phase as one goes up in height where Z_{DR} drops from a peak of ~1.5 dB to a minimum of 0 dB.

shown in Fig. 1 caused extensive damage to Greeley, Colorado, 1/2 hour earlier; surface observations of baseball-sized hail were reported by mobile observers with the Prototype Regional Observing and Forecasting Systems of the National Oceanic and Atmospheric Administration (NOAA). Observers were located at the points marked A and B in Fig. 1. Regions of larger positive Z_{DR} surrounding the hail cell are locations where rain fell.

On the evening of 8 June 1983, a severe storm developed near Wiggins, Colorado. Low-elevation PPI scans of Z_H and Z_{DR} are shown in Fig. 2, a and b, respectively. Locations of three hail cells based on the Z_{DR} hail signal are contoured in Fig. 2. Note the clear delineation of hailshafts from rain regions. A range height indicator (RHI) scan at an azimuth of 76° through the same storm at a slightly later time is shown in Fig. 3. The center of the hailshaft occurs approximately at 80-km range, where $Z_H > 55$ dBZ and $Z_{DR} \cong 0$ dB. Regions of rainfall surround the hailshaft and are characterized by $Z_{DR} \gtrsim 0.5$ dB. Note also the discrimination between ice and water phase with height observed with the Z_{DR} signal, a characteristic signature (*23*).

The Z_{DR} radar technique is likely to become an important procedure for the detection of hail in severe storms and in hail suppression research. Although further work is required to demonstrate the utility of this technique in an operational environment, a preliminary assessment based upon the results of Project MAYPOLE and other experiments strongly supports use of the Z_{DR} technique for this purpose (*22, 24*).

V. N. BRINGI
Department of Electrical Engineering, Colorado State University, Fort Collins 80523

THOMAS A. SELIGA
KULTEGIN AYDIN
Atmospheric Sciences Program and Department of Electrical Engineering, Ohio State University, Columbus 43210

References and Notes

1. B. Cook, *Mon. Weather Rev.* **86**, 435 (1958); R. H. Douglas and W. Hitschfeld, Science Report MW-27 (Stormy Weather Group, McGill University, Montreal, 1958); R. J. Donaldson, Jr., A. C. Chmela, C. R. Shackford, in *Physics of Precipitation* (American Geophysical Union, Washington, D.C., 1959), pp. 354–369; R. J. Donaldson, Jr., *J. Meteorol.* **18**, 292 (1961).
2. P. J. Petrocchi, Science Report AFGL-TR-82-0277 (Air Force Geophysics Laboratory, Hanscom Air Force Base, Mass., 1982).
3. R. J. Donaldson, Jr., and D. W. Burgess, in *Proceedings of the NEXRAD Doppler Radar Symposium/Workshop*, P. S. Ray and K. Colbert, Eds. [University of Oklahoma (Norman)–NOAA, Washington, D.C., 1982], pp. 102–123.
4. D. Atlas and F. H. Ludlam, *Q. J. R. Meteorol. Soc.* **87**, 523 (1961).
5. G. K. Sulakvelidze, N. Sh. Bibilashvili, V. F. Lapcheva, *Formation of Precipitation and Modification of Hail Processes* (Israel Program for Scientific Translation, Jerusalem, 1965); G. K. Sulakvelidze, B. I. Kiziriya, V. V. Tsykunov, in *Weather and Climate Modification*, W. N. Hess, Ed. (Wiley, New York, 1974), pp. 410–431; I. I. Burtsev, *Modification of Hail Processes* (Gidrometeoizdat, Leningrad, 1973).
6. D. Atlas, *Adv. Geophys.* **10**, 317 (1964).
7. P. J. Eccles and D. Atlas, *J. Appl. Meteorol.* **12**, 847 (1973).
8. R. E. Rinehart and J. D. Tuttle, *ibid.* **21**, 1865 (1982).
9. G. C. McCormick and A. Hendry, *Radio Sci.* **10**, 421 (1975).
10. B. L. Barge, Science Report MW-71 (Stormy Weather Group, McGill University, Montreal, 1972); G. C. McCormick, L. E. Allan, A. Hendry, *J. Appl. Meteorol.* **18**, 77 (1979); A. Hendry and Y. M. M. Antar, *Radio Sci.* **19**, 115 (1984).
11. R. G. Humphries, thesis, McGill University (1974); Science Report MW-82 (Stormy Weather Group, McGill University, Montreal, 1974); J. I. Metcalf, *Radio Sci.* **16**, 1373 (1981); T. A. Seliga, K. Aydin, V. N. Bringi, *ibid.* **19**, 81 (1984).
12. T. A. Seliga and V. N. Bringi, *J. Appl. Meteorol.* **15**, 69 (1976).
13. R. G. Knollenberg, *ibid.* **9**, 86 (1970).
14. V. N. Bringi, T. A. Seliga, W. A. Cooper, *Radio Sci.* **19**, 157 (1984); W. A. Cooper, V. N. Bringi, V. Chandrasekhar, T. A. Seliga, in Preprints, 21st Conference on Radar Meteorology, Edmonton, Alberta (American Meteorological Society, Boston, 1983), pp. 488–493.
15. G. C. McCormick, A. Hendry, B. L. Barge *Nature (London)* **238**, 214 (1972); K. V. Beard and A. R. Jameson, *J. Atmos. Sci.* **40**, 448 (1983).
16. A. Hendry, G. C. McCormick, B. L. Barge, *J. Appl. Meteorol.* **15**, 635 (1976).
17. H. R. Pruppacher and K. V. Beard, *Q. J. R. Meteorol. Soc.* **96**, 247 (1970); H. R. Pruppacher and R. L. Pitter, *J. Atmos. Sci.* **28**, 86 (1971).
18. A. Hendry and Y. M. M. Antar, *Radio Sci.* **19**, 115 (1984).
19. S. Richardson, B. Barge, R. Humphries, in Preprints, 21st Conference on Radar Meteorology, Edmonton, Alberta (American Meteorological Society, Boston, 1983), pp. 421–424.
20. V. N. Bringi, T. A. Seliga, S. M. Cherry, *IEEE Trans. Geosci. Remote Sensing* **21**, 215 (1983).
21. V. N. Bringi and T. A. Seliga, *Ann. Telecommun.* **32**, 392 (1977); T. A. Seliga and V. N. Bringi, *Radio Sci.* **13**, 271 (1978); K. Aydin and A. Hizal, Union Radio Scientifique Internationale (URSI) National Radio Science Meeting Abstracts, Seattle, Wash., June 1979.
22. T. A. Seliga, K. Aydin, C. P. Cato, V. N. Bringi, in *Cloud Dynamics*, E. M. Agee and T. Asai, Eds. (Reidel, Dordrecht, 1982), pp. 285–300; K. Aydin, T. A. Seliga, V. N. Bringi, *Radio Sci.* **19**, 58 (1984).
23. M. P. M. Hall, S. M. Cherry, J. W. F. Goddard, G. R. Kennedy, *Nature (London)* **285**, 195 (1980).
24. V. N. Bringi, V. Chandrasekhar, T. A. Seliga, P. L. Smith, R. Hari, in Preprints, 21st Conference on Radar Meteorology, Edmonton, Alberta (American Meteorological Society, Boston, 1983), pp. 494–499; M. J. Leitao and P. A. Watson, *Radio Sci.* **19**, 209 (1984).
25. This work was supported by the Atmospheric Research Section, National Science Foundation, under grants ATM-8003376 and ATM-8117045, and by the Army Research Office through the University Corporation for Atmospheric Research subcontracts NCAR S3024 and NCAR S3025. We are grateful to R. E. Carbone, P. H. Herzegh, and other staff members of the Field Observing Facility (NCAR), for their assistance in the conduct of this research during Project MAYPOLE. Cooperation of the mobile observers with NOAA's Prototype Regional Observing and Forecasting Systems group in verifying the hail observations on 4 June 1983 is gratefully acknowledged. Software support for radar data analysis was provided by C. Mohr and L. J. Miller of the Convective Storms Division, NCAR. NCAR is sponsored by the National Science Foundation.

23 February 1984; accepted 10 April 1984

Large Yearly Production of Phytoplankton in the Western Bering Strait

Abstract. *Production in the western Bering Strait is estimated at 324 grams of carbon per square meter per year over 2.12×10^4 square kilometers. An ice-reduced growing season makes this large amount of primary production unexpected, but it is consistent with the area's large upper trophic level stocks. The productivity is fueled by a cross-shelf flow of nutrient-rich water from the Bering Sea continental slope. This phytoplankton production system from June through September is analogous to a laboratory continuous culture.*

Mesoscale spatial patterns in marine productivity usually reflect underlying physical processes that determine phytoplankton growth conditions. In low latitudes, surface divergence is necessary to bring nutrient-containing water into euphotic depths. In high-latitude cold surface waters, nutrients increase during winter when mixed layer light conditions are poor and are seasonally incorporated into plant organic material only under suitable upper water column light and mixing conditions (*1*). Despite these limitations, intense summer productivity in the western Bering Strait creates a large amount of phytoplankton each year.

The eastern Bering Sea is unusual among continental shelves because of its large area and a cross-shelf advection into the Arctic Ocean through the Bering Strait (Fig. 1). Current measurements suggest average flow through the Bering Strait is approximately 0.8 sverdrups (*2*). This flow is seasonal, being greater in summer because of the higher frequency of flow reversals in winter. The water passing through the strait has three major components (*3*). In the west, the flow is dominated by cold, high salinity water from the Gulf of Anadyr. This flow appears to be a continuation of the shelf break current that turns north near Cape Navarin (Fig. 1). In the east, warmer coastal water dominated by Yukon River discharge flows out of Norton Sound. South of Saint Lawrence Island, the third water mass (modified shelf water) is formed. The Bering shelf–Anadyr water in the west and the Alaskan coastal–Yukon River water in the east maintain their identity during transit through the strait.